HHS Public Access

Author manuscript

Clin Cancer Res. Author manuscript; available in PMC 2015 May 19.

Published in final edited form as:

Clin Cancer Res. 2011 April 15; 17(8): 2301–2313. doi:10.1158/1078-0432.CCR-10-3077.

A novel HSP90 inhibitor delays castrate resistant prostate cancer without altering serum PSA levels and inhibits osteoclastogenesis

Francois Lamoureux[1], **Christian Thomas**[1], **Min-Jean Yin**[2], **Hidetoshi Kuruma**[1], **Ladan Fazli**[1], **Martin E Gleave**[1], and **Amina Zoubeidi**[1]

[1]The Vancouver Prostate Centre, University of British Columbia, Vancouver, BC, Canada

[2]Pfizer Worldwide Research & Development, Oncology Research, San Diego, CA, United States

Abstract

Purpose—Prostate cancer responds initially to anti-androgen therapies, however, progression to castration resistant disease frequently occurs. Therefore there is an urgent need for novel therapeutic agents that can prevent the emergence of castration resistant prostate cancer (CRPC). Hsp90 is a molecular chaperone involved in the stability of many client proteins including Akt and androgen receptor (AR). 17-AAG have been reported to inhibit tumor growth in various cancers, however induces tumor progression in the bone microenvironment.

Methods—Cell growth, apoptosis, and AR transactivation were examined by crystal violet assay, flow cytometry and luciferase assays respectively. The consequence of HSP90 therapy *in vivo* was evaluated in LNCaP xenograft model. The consequence of PF-04928473 therapy on bone metastasis was studied using an osteoclastogenesis *in vitro* assay.

Results—PF-04928473 inhibits cell growth in a panel of prostate cancer cells, induces cell cycle arrest at sub-G1 and leads to apoptosis and increased caspase-3 activity. These biologic events were accompanied by decreased activation of Akt and Erk as well as decreased expression of Her2, and decreased AR expression and activation *in vitro*. In contrast to 17-AAG, PF-04928473 abrogates RANKL-induced osteoclast differentiation by affecting NF-kB activation and Src phosphorylation. Finally, PF-04929113 inhibited tumor growth and prolonged survival compared to controls. Surprisingly, PF-04929113 did not reduce serum PSA levels *in vivo* in parallel these decreases in tumor volume.

Conclusion—These data identify significant anti-cancer activity of PF-04929113 in CRPC but suggest that serum PSA may not prove useful as pharmaco-dynamic tool for this drug.

Keywords

HSP90 inhibitor; Androgen Receptor; PSA; Castration-Resistant Prostate Cancer

Corresponding author: Dr. Amina Zoubeidi, The Vancouver Prostate Centre, 2660 Oak Street, Vancouver, BC, V6H 3Z6, Canada, azoubeidi@prostatecentre.com.

Introduction

Prostate cancer is the most common cancer and the third most common cause of cancer related mortality in men in the United States (1). Hormonal therapy remains the most effective therapy for patients with advanced prostate cancer, inhibiting proliferation and inducing apoptosis in tumor cells (2). Unfortunately, after short-term remissions (18–24 months), surviving tumor cells recur with castrate resistant prostate cancer (CRPC) with inevitable progression and death within 2 to 3 years in most men (3, 4). CRPC progression is a process by which tumor cells acquire the ability to both survive in the absence of androgens and proliferate using non-androgenic stimuli for mitogenesis. To significantly improve survival in men with prostate cancer, new therapeutic strategies to inhibit the appearance of this phenotype must be developed.

Heat shock protein 90 (Hsp90) is an ATPase-dependent molecular chaperone (5) required for protein folding, maturation and conformational stabilization of many “client” proteins, protecting them from aggregation (6). Indeed, Hsp90 interacts with several client proteins regulating proliferation and cell survival of tumor cells, including growth factor receptors, cell cycle regulators and signaling kinases such as Akt or Raf-1 (7–9). Tumor cells exhibit higher HSP90 activity and expression compared with normal cells (6, 10). AR is a known client protein of Hsp90 (11) and plays a key role in prostate carcinogenesis and progression even in CRPC. Hsp90 inhibition has been shown to disrupt nuclear localization of the AR (12). Consequently, Hsp90 inhibition represents an exciting strategy as a new treatment for CRPC. To date, many Hsp90 inhibitors targeting the ATPase pocket have been developed, including natural compounds like geldanamycin and its analog 17-allylamino-17-demethoxy-geldanamycin (17-AAG), inducing apoptosis in preclinical studies of colon, breast, and prostate cancer (6, 13–15). However, 17-AAG contains a benzoquinone moiety that can cause liver toxicity (16), and is poorly soluble leading to formulation challenges and additional toxicities that has limited its clinical development. Added to this, 17-AAG has been reported to potentiate tumor growth in bone by inducing osteoclastogenesis in murine breast and prostate cancer models, and hence raises concerns in patients with bone metastasis (17, 18).

PF-04928473 (SNX-2112) is a nonquinone-based Hsp90 inhibitor that competitively binds to the N-terminal adenosine trisphosphate-binding site of Hsp90 (19, 20). It can be orally delivered via its pro-drug PF-04929113 (SNX-5422) and converted into PF-04928473 which is extremely potent against various cancers (19, 20). In the present study, we elucidated the mechanistic and *in vitro* anti-cancer activity of PF-04928473. *In vivo* experiments were designed to study the effects of PF-04929113 on tumor progression and animal survival in LNCaP castrate-resistant prostate cancer model. Furthermore, we investigated the effects of PF-04928473 on osteoclastogenesis *in vitro* in pre-osteoclast cells.

Materials and Methods

Tumor cell lines and reagents

The human prostate cancer cell lines PC-3, PC-3-M and DU145, were purchased from the American Type Culture Collection (2008 and 1989, ATCC-authentication by isoenzymes

analysis) and maintained in DMEM (Invitrogen-Life Technologies, Inc.) supplemented with 5% fetal bovine serum and 2mmol/L L-glutamine. LNCaP and C4-2 cells were kindly provided by Dr. Leland W.K. Chung (1992, MDACC, Houston Tx) and tested and authenticated by whole-genome and whole-transcriptome sequencing on Illumina Genome Analyzer IIx platform in July 2009. C4-2 and LNCaP cells were maintained RPMI 1640 (Invitrogen Life Technologies, Inc.) supplemented with 5% fetal bovine serum and 2mmol/L L-glutamine. All cell lines were cultured in a humidified 5% CO_2/air atmosphere at 37°C. All cell lines were passaged for less than 3 months after resurrection. Western blotting and/or real time PCR was performed for AR and PSA each time when LNCaP or C4-2 cells were resurrected.

Hsp90 Inhibitors

Hsp90 inhibitors, PF-04928473 (4-(6,6-Dimethyl-4-oxo-3-trifluoromethyl-4,5,6,7-tetrahydro-indazol-1-yl)-2-(4-hydroxy-cyclohexylamino)-benzamide) and its pro-drug PF-04929113, orally bioavailable, were kindly provided from Pfizer (La Jolla, CA) and used for *in vitro* and *in vivo* studies, respectively. These compounds are synthetic small molecule inhibitors that bind the N-terminal adenosine triphosphate binding site of Hsp90. For the *in vitro* studies, PF-04928473 was dissolved in dimethyl sulfoxide (DMSO) at 10 mM stock solutions and stored at −20°C. For the *in vivo* studies, PF-04929113 was dissolved in PBS 1% carboxymethylcellulose and 0.5% Tween 80 (Invitrogen-Life Technologies, Inc.) at 15 mg/ml and stored at 4°C.

Cell proliferation and apoptosis assays

Prostate cells lines were plated in media DMEM or RPMI with 5% of FBS and treated with PF-04928473 at indicated concentration and time. After time course exposure, cell growth was measured using the crystal violet assay, as described previously (21). Detection and quantitation of apoptotic cells were done by flow-cytometry (described below) and western blotting analysis. Each assay was repeated in triplicate.

Caspase 3 activity was assessed three days after treatment using the Fluorometric CaspACE Assay System, (Promega, Madison, WI, USA). Fifty μg of total cell lysate were incubated with caspase-3 substrate AC-DEVD-AMC at room temperature for 4 hours. Caspase-3 activity was quantified in a fluorometer with excitation at 360nm and emission 460nm.

Cell cycle analysis

Prostate cancer cell lines were incubated with or without 1μM PF-04928473 for 24, 48, 72 or 96 hrs, trypsinized, washed twice and incubated in PBS containing 0.12% Triton X-100, 0.12 mM EDTA and 100 μg/ml ribonuclease A. 50 μg/ml propidium iodide was then added to each sample for 20 min at 4°C. Cell cycle distribution was analyzed by flow cytometry (Beckman Coulter Epics Elite, Beckman, Inc., Miami, FL), based on 2N and 4N DNA content. Each assay was done in triplicate.

Western blotting analysis

Samples containing equal amounts of protein (depending on the antibody, 5–50μg) from lysates of cultured tumor prostate cell lines underwent electrophoresis on SDS-

polyacrylamide gel and were transferred to nitrocellulose filters. The filters were blocked in Odyssey Blocking Buffer (LI-COR Biosciences) at room temperature for 1 h. And then, blots were probed overnight at 4°C with primary antibodies (supplementary materials) to detect proteins of interests. After incubation, the filters were washed x3 with washing buffer (PBS containing 0.1% Tween) for 5 min. Filters were then incubated for 1 h with 1:5,000 diluted Alexa Fluor secondary antibodies (Invitrogen) at room temperature. Specific proteins were detected using ODYSSEY IR imaging system (LI-COR Biosciences) after washing, as described above.

Quantitative Reverse Transcription-PCR

Total RNA was extracted from cultured cells after 48 hours of treatment using TRIzol reagent (Invitrogen Life Technologies, Inc.). Two μg of total RNA was reversed transcribed using the Transcriptor First Strand cDNA Synthesis Kit (Roche Applied Science). Real time monitoring of PCR amplification of complementary DNA (cDNA) was performed using DNA primers (supplemental table) on ABI PRISM 7900 HT Sequence Detection System (applied Biosystems) with SYBR PCR Master Mix (Applied Biosystems). Target gene expression was normalized to GAPDH levels in respective samples as an internal standard, and the comparative cycle threshold (Ct) method was used to calculated relative quantification of target mRNAs. Each assay was performed in triplicate.

Transfection and luciferase assay

LNCaP and C4-2 cells ($2.5x10^5$) were plated on six-well plates and transfected using lipofectin (6μL per well; Invitrogen Life Technologies, Inc.). The total amount of PSA or NF-KB plasmids DNA used were normalized to 1μg per well by the addition of a control plasmid. Media were replaced by charcoal-stripped serum (CSS) ± PF-04928473 for 24h ± 0.1nM R1881 for 12h to activate AR or ± 20ng/ml TNF-α to activate NF-KB. PSA- or NF-KB-luciferase activities were measured using Dual-Luciferase Reporter Assay System (Promega) with the aid of a microplate luminometer (EG&G Berthold). All experiments were carried out in triplicate wells and repeated 3 times using different preparations of plasmids.

Immunofluorescence

LNCaP and C4-2 cells were grown on coverslips and treated with different concentrations of PF-04928473 for 48 hours and then treated ± 1 nM R1881 for 6 hours. After treatment, cells were fixed in ice-cold methanol completed with 3% acetone for 10 min at −20°C. Cells were the washed thrice with PBS and incubated with 0.2% Triton/PBS for 10 min, followed by washing and 30 min blocking in 3% nonfat milk before the addition of antibody overnight to detect AR (1:250). Antigens were visualized using anti-mouse antibody coupled with FITC (1:500; 30 min). Photomicrographs were taken at 20X magnification using Zeiss Axioplan II fluorescence microscope, followed by analysis with imaging software (Northern Eclipse, Empix Imaging, Inc.).

Cell culture and osteoclast differentiation assays

Murine RAW 264.7 monocytic cells (American Type Culture Collection) were cultured in phenol red-free alpha-MEM (Invitrogen Life Technologies, Inc.) supplemented with 10% fetal bovine serum (FBS), and 1% nonessential amino acids (Invitrogen Life Technologies, Inc.). To induce osteoclast formation, RAW 264.7 cells were scraped and incubated at 37°C for 2 min to allow adherence of the more differentiated cells. Nonadherent cells were then seeded in fresh medium at 3 x 10^3 or 10 x 10^3 cells in 96- or 24-well plates. After 2 h, the cells were treated with 100 ng/ml recombinant human RANKL (R&D) with or without PF-04928473 or 17-AAG at indicated concentration, for 5 days. Multinucleated cells were counted under a light microscope after May Grünwald/Giemsa (MGG) staining (Sigma) or tartrate-resistant acid phosphatase (TRAP) staining (Leukocyte Acid Phosphatase Assay kit; Sigma). All experiments were performed in triplicate at least three times.

Animal Treatment

Male athymic mice (Harlan Sprague-Dawley, Inc.) were injected subcutaneous with 2 x 10^6 LNCaP cells (suspended in 0.1 mL Matrigel; BD Biosciences) and castrated once tumors reach 300 – 500mm^3 or when serum PSA increased above 50 ng/mL. Once tumors were progressed to castrate resistance, mice were randomly assigned to vehicle or PF-04929113 (50 mg/kg; formulation in 0.5% CMC + 0.5% Tween-80) and treated orally three times per week. Each experimental group consisted of 8 mice. Tumor volume and PSA measurements were performed twice and once weekly, respectively. Tumor volume was calculated by the formula: length x width x depth. Serum PSA measurements were performed by enzymatic immunoassay (ClinPro International Co. LLC, Union City, USA). Data points were expressed as average tumor volume ± SE or average PSA concentration ± SE. After sacrifice (when the tumor volume reached ≥ 10% of body weight), tumors were harvested for evaluation of protein expression by western blotting analyses and immunohistochemistry. All animal procedures were performed according to the guidelines of the Canadian Council on Animal Care and appropriate institutional certification.

Immunohistochemistry

Immunohistochemistry was performed on formalin-fixed, paraffin-embedded 4 μm sections of tumor samples. Immunohistochemical staining was conducted using a primary antibody (supplementary materials) in the Ventana autostainer Discover XT (Ventana Medical System) with enzyme labeled biotin streptavidin system and solvent resistant 3,3′-diaminobenyidine Map kit. All comparisons of staining intensities were made at 200x magnifications.

Statistical analysis

All *in vitro* data were assessed using the Student t test and Mann-Whitney test. Tumor volumes of mice were compared using Kruskal-Wallis test. Overall survival was analyzed using Kaplan-Meier curves. Levels of statistical significance were set at $P < 0.05$.

Results

PF-04928473 inhibits prostate cancer cell proliferation

Figure 1A illustrates the chemical structure of PF-04928473 (active molecule) and PF-04929113 (pro-drug). We first assessed the effects of PF-04928473 and 17-AAG on cell growth in several prostate cancer cell lines (PC3, PC3-M, DU145, LNCaP and C4-2) using a crystal violet assay. In all cancer cell lines tested, PF-04928473 inhibited cell growth in dose-dependent manner, with IC_{90} at 72 hours values ranged from 6.5 to 42nM (LNCaP: 6.5nM; C4-2: 8.2nM; DU-145: 16nM; PC-3: 36nM and PC-3-M: 42nM; Fig 1B)and IC_{50} values ranged from 13.5 to 95nM (LNCaP: 19.5nM; C4-2: 13.5nM; DU-145: 43nM; PC-3: 50 nM and PC-3-M: 95nM; Fig 1B). Compared to 17-AAG, PF-04928473 was more potent in all cell lines except C4-2. Moreover, LNCaP and C4-2 cells, which express the AR, are at least 2 fold more sensitive to PF-04928473 than the other AR-negative cell lines (PC-3, PC-3-M and DU-145). Subsequent experiments focused on LNCaP and C4-2 androgen-sensitive cell lines. Because IGF-1 and IL-6 play important roles in the proliferation of prostate tumor cells, we investigated whether PF-04928473 suppresses the proliferation induced by these cytokines. PF-04928473 significantly inhibits cancer cell proliferation induced by IL-6 or IGF-1 (Fig S1B, $P < 0.001$). These results demonstrate that Hsp90 inhibition using PF-04928473 potently inhibits tumor cell proliferation induced by cytokine, IL-6 and IGF-1.

PF-04928473 induces apoptosis in prostate tumor cell lines

We next assessed the effects of Hsp90 inhibition on prostate cancer cell apoptosis using flow-cytometric and western blot analyses. The fraction of cells undergoing apoptosis (sub G1 fraction) significantly increased in a time-dependent manner with PF-04928473 compared to control in both LNCaP (88% after 96 hours vs 3% in control, $P < 0.001$; Fig 1C left) and C4-2 cells (Fig S2). Consequently, the G_0/G_1, S, and G_2/M fractions were significantly reduced in a time-dependent manner, accompanied by decreased levels of cell cycle proteins, CDK4 and cyclin D1 (Fig 1C right). Furthermore, PF-04928473 induced caspase-3 activation in a dose-dependent manner as shown by both increased cleaved caspase 3 by western blot analysis (Fig 1D right) and CaspACE Assay System ($P < 0.001$; Fig 1D left). These results suggest that PF-04928473 induces apoptosis in a caspase 3 dependent manner.

PF-04928473 down-regulates Hsp90 client proteins but up-regulates several Heat Shock Proteins (HSPs) in prostate cancer cell lines

Inhibition of Hsp90 causes proteasomal degradation of a subset of cellular proteins. We investigated the effect of PF-04928473 on Hsp90-protein client and others HSPs. Expression of Hsp90, Hsp70, Hsp27 and clusterin as markers of HSF-1-dependent stress response (22, 23), were increased by PF-04928473 in a dose- and a time-dependent manner in LNCaP cells (Fig 2A) and all other prostate cancer cell lines tested (Fig S2). These results show a typical HSF-1 stress response following Hsp90 inhibition and also demonstrate for the first time that clusterin can be considered a stress biomarker like Hsp70 after treatment with an Hsp90 inhibitor. P23, a protein required in the Hsp90 complex, was degraded in a dose- and a time-dependent manner in LNCaP and C4-2 cells (Fig 2A and S2), confirming inhibition

of the Hsp90 complex. PF-04928473 also decreased levels of various Hsp90 client proteins, including Akt, ERK, p-ERK and Her2 and (Fig 2A and S2).

PF-04928473 inhibits AR pathway by its degradation in prostate cell lines

We next evaluated the effects of PF-04928473 on AR levels and activity in LNCaP and C4-2cells. PF-04928473 induced AR degradation as shown by western blotting analysis, and consequently decreased PSA protein levels (Fig 2A). Similar results were seen in C4-2 cells (Fig S3). Additionally, PF-04928473 significantly abrogated R1881-induced AR-mediated gene activation as shown by a decrease PSA-luciferase activity at concentrations as low as 10 nM (± 1.7 fold, $P < 0.001$) in LNCaP (Fig 2B) and C4-2 (Fig S3) cells. Quantitative RT-PCR indicated that PF-04928473 does not alter AR mRNA levels, but does significantly decrease mRNA levels of target genes of AR: PSA, NKX3.1 and FKBP5 (Fig 2C). AR localization was also altered after treatment with PF-04928473. While abundant AR resides in the nucleus following R1881 treatment (Fig 2D), nuclear staining of AR was lost and only weak cytoplasmic staining was identified after treatment with PF-04928473. Similar results were obtained in C4-2 cells (Fig S3).

PF-04929113 inhibits castrate resistant LNCaP tumor growth

In light of the potent inhibitory *in vitro* effects of PF-04928473 on prostate tumor cell lines, we next tested the effects of PF-04929113 on castrate-resistant LNCaP tumor growth. Mice bearing LNCaP tumors were castrated when PSA values exceeded 50 ng/ml, and when PSA increased back above pre-castration levels, mice were treated three times per week with 50 mg/kg PF-04929113 orally. All animals treated with PF-04929113 (n=8) exhibited a significant decrease in tumor volume compared with control mice starting at the day 17 (240mm^3 and 1293.9mm^3, respectively) and after 45 days (459.2mm^3 and 2818.2mm^3, respectively; Fig. 3A). When each animal is considered individually, the incidence of mice progressing with a tumor volume ≥ 500mm^3 was significantly diminished by day 22 in PF-04929113-treated animals (0/8) compared with controls (8/8, Fig 3B). Rate of tumor progression at days 10 and 45 was also significantly decreased (1947.8mm^3 for control mice vs 244.1mm^3 for treated mice, $p<0.001$) in the treatment group, compared with control mice (Fig 3C). Consequently, progression-free ($p<0.001$) and cancer specific ($p<0.001$) survival were significantly prolonged in the PF-04929113-treated group (Fig 3D). Indeed, by day 60, all mice were euthanized due to a high tumor burden in the vehicle group, while all mice were still alive in the PF-04929113-treated group. These data demonstrate that targeting Hsp90 by PF-04929113 significantly inhibits castrate resistant tumor growth and prolongs survival in the LNCaP tumor model.

Immunohistochemical analysis indicated increased Hsp70 expression, and decreased Ki67, Akt, and AR expression, after treatment with PF-04929113 (Fig 4A). All results were confirmed by quantitative real-time PCR (data not shown), and by western blotting (Fig 4B). Inhibition of tumor progression by PF-04929113 may result from a combination of decreased proliferative (reduced Ki67 and Akt expression) or increased apoptosis (increased apoptag staining) rates (Fig 4).

Serum PSA does not correlate with tumor volume changes after PF-04929113 treatment

Fig. 5C illustrates the relationship between serum PSA and tumor volume in control or treated mice. While mean serum PSA levels were lower in the PF-04929113 group compared with control mice (Fig 5A and B), PF-04929113 treatment did not reduce circulating PSA level in parallel with changes in tumor volume. In controls, as previously reported (24), serum PSA levels increase proportionally with increases in tumor volume with a high degree of correlation ($r=0.7233$, Fig 5C), In contrast, in PF-04929113-treated mice, serum PSA correlated poorly with tumor volume ($r=0.4694$, $p<0.001$, Fig 5C), being higher than expected on a per-volume basis in this group. Fig 5D illustrates kinetics of serum PSA and corresponding tumor volume of mice treated after 75 days of PF-04929113. During treatment, mean PSA levels increased from 70ng/ml to 1000ng/ml while mean tumor volume remained stable up to day 60. Interestingly, when PF-04929113 treatment was stopped, serum PSA levels decreased 5 fold over 25 days while tumor volume increased. These *in vivo* data indicate that serum PSA correlates poorly with CRPC progression, and may be enhanced during PF-04929113 treatment. This *in vivo* finding was particularly surprising, considering that *in vitro* treatment with PF-04928473 caused AR degradation and reduced PSA expression levels (Fig 2). Consequently, serum PSA may not a good biomarker for Hsp90 inhibition.

PF-04928473 inhibits osteoclastogenesis

Because 17-AAG has been reported to induce osteoclastogenesis and consequently stimulate tumor progression in bone environments (17, 18), we next investigated the effect of PF-04928473 on osteoclastogenesis. Raw 264.7 cells were cultured with 100ng/mL RANKL for 5 days, in presence of 10nM or 500nM of PF-04928473 or 17-AAG. PF-4928473 potently inhibited osteoclast formation from Raw 264.7 pre-osteoclast cells cultured in presence of RANKL, whereas 17-AAG significantly induced osteoclast formation alone (500nM) or in presence of RANKL at the indicated concentrations (Fig 6A). Since activation of NF-κB is an essential step for osteoclast differentiation (25), we compared luciferase-NF-κB activity in presence of 17-AAG and PF-04928473 in Raw 264.7 cells to explain differences of osteoclastogenesis between these two Hsp90 inhibitors. Compared to 17-AAG, PF-04928473 significantly decreased luciferase-NF-κB activity in osteoclast precursors (Fig. 6B). Because Src kinase is reported to be essential for osteoclast maturation (26, 27) and is activated shortly after 17-AAG treatment (18), we next compared Src activation by PF-04928473 or 17-AAG. Phospho-Src was rapidly and significantly increased within 1h after treatment with 17-AAG ($p<0.05$; Fig 6C), while PF-04928473 significantly decreased p-Src in Raw 264.7 cells cultured in presence of RANKL ($p<0.01$; Fig 6C). Total Src was not changed during the treatment.

Discussion

Most treatments for CRPC have been approved for symptomatic benefit, such as mitoxantrone chemotherapy, the bisphosphonate zoledronic acid, and radioactive isotopes. Only docetaxel, and more recently, cabazitaxel and abiraterone, have been shown to improve overall survival. New treatments, preferably based on selective targeting of mechanistically relevant cancer proteins, are urgently needed for patients with advanced -

disease. Hsp90 is an attractive therapeutic target because as a molecular chaperone it guides the normal folding, stability, maturation and activity of many client proteins critical for cell survival. Cancer cells are particularly sensitive to Hsp90 inhibition because many client proteins play critical roles in oncogenesis. Several Hsp90 such as 17-AAG and other novel ansamycins including the orally bioavailable geldanamycin derivative 17-(dimethylaminoethylamino)-17 demethoxygeldanamycin and the soluble pro-drug of 17-DMAG are already in clinic (28, 29). But these drugs necessitate complex formulations associated with limited bioavailability and hepatotoxicity (30).

Owing to these limitations of the ansamycin-derived Hsp90 inhibitors, we examined the effects of a novel HSP90 inhibitor, PF-04928473 and its pro-drug, PF-04929113, in prostate tumor cell lines and castrate-resistant LNCaP xenograft model. PF-04928473 binds the ATP pocket and thereby inhibits many Hsp90 client proteins and downstream target genes. *In vitro*, PF-04928473 demonstrated superior potency in a panel of prostate cell lines compared to 17-AAG, inducing apoptosis and degradation of client proteins, such as Her2, AR, Akt and ERK, in a dose-dependent manner in prostate tumor cell lines.

PF-04928473 has a high oral bioavailability with good solubility delivered via its pro-drug PF-04929113 and is active in various preclinical cancer cell lines and models (19, 20). We found that PF-04929113 significantly delayed tumor growth of castrate-resistant LNCaP xenografts and prolonged cancer-specific free survival. After 60 days of treatment all 8 mice in the treatment group were still alive, whereas all 8 control mice died or required sacrifice. No side effects or toxicity were observed after treatment with PF-04929113, in contrast to reports of hepatotoxicity with 17-AAG (30). PF-04929113 decreased Ki67 expression, increased apoptotic rates, decreased levels of Hsp90 client proteins such as Akt (15, 31), and increased of Hsp70 in tumors *in vivo* as previously documented (15, 31).

Bone metastasis is associated with significant morbidity and mortality in advanced prostate cancer, affecting more than 80% of CRPC patients (32). Quinn et *al.* identified that Hsp90 expression correlates with bone metastasis in an *in vivo* mouse model (33). Also, c-Src and other Hsp90 client proteins like matrix metalloproteinase-2 (MMP2) or epidermal growth factor receptor (EGFR) lead to bone metastasis by differentiation and activation of osteoclasts (34, 35). Conflicting reports suggest that Hsp90 inhibition may inhibit both primary tumor growth and bone tumor metastasis (36, 37), while several more recent studies have reported that Hsp90 inhibition using 17-AAG promotes prostate and breast cancer growth in bone by mechanisms involving osteoclast differentiation and activation (17, 18). These results a potential risk to use 17-AAG therapies in patients with bone metastasis. In this report, we observed induction of osteoclastogenesis with 17-AAG while the opposite effect was observed with PF-04928473, which abrogates RANKL-induced osteoclast differentiation and is associated with downregulation of NF-κB activity. The classical NF-κB pathway is known to play a pivotal role in osteoclast formation, function, and survival (38, 39). Indeed, the double knock down of NF-κB causes an osteopetrotic phenotype with growth retardation and craniofacial abnormalities in mice (40). Our results show that, in contrast to 17-AAG, PF-04929113 inhibits key proteins involved in osteoclastogenesis, such as p-Src and Akt.

LNCaP tumors secrete PSA, express AR, and relapse after androgen ablation therapy, mimicking many aspects of CRPC including intratumoral androgen synthesis (41), increased expression of stress-activated molecular chaperones (CLU, Hsp27), re-activation of the AR (42), and rising AR-driven serum PSA levels (24). The LNCaP model shows an accurate correlation between tumor volume and serum PSA levels and undergoes an 80% decrease of PSA after castration (24). PSA is considered the most useful biomarker in prostate cancer (43) and used as a clinically useful tool in the follow-up of patients post treatment. Several clinical investigations indicate that the serum PSA levels are roughly proportional to tumor volume and stage (44, 45). In reported *in vitro* studies, inhibition of Hsp90 induced degradation of the AR associated with a decrease of PSA expression (15, 46, 47). No *in vivo* data was reported. In the present study, we found that serum PSA levels continued to climb with PF-04929113 despite significant delays in tumor growth of castrate-resistant LNCaP xenografts, highlighting that serum PSA level does not always correspond with clinical response as reported in human patients (48, 49). PF-04929113 induces a significant decrease of AKT and a slight reduction of AR expression in tumor tissues, whereas the drug completely reduces AR and PSA expressions *in vitro.* One explaination for the discrepancy between *in vitro* and *in vivo* data is that, compared to AR, AKT is inhibited at lower concentrations of PF-04929113, and the concentration of PF-04929113 used *in vivo* is not enough to suppress AR-driven PSA levels. There were conflicting data in the literature on the crosstalk between PI3K/AKT and AR signaling pathways. AKT pathway was recently reported to be dominant over AR signaling in prostate cancer cells (50). Indeed, the authors suggest that the inhibition of PI3K/AKT signaling activates AR transactivation potential (50). This hypothesis could explain the *in vivo* results without inhibition of PSA level, in spite of the opposite *in vitro* data. Consequently, serum PSA does not reflect the anti-cancer activity to monitor response to HSP90 inhibition *in vivo*.

In summary, these data identify significant anti-cancer effects of the Hsp90 inhibitor, PF-04929113, in a model of CRPC, and that unlike 17-AAG analogues, is not associated with src activation and osteoclastogenesis. However PSA should not be considered as a pharmaco-dynamic marker of on-target inhibition or anti-cancer activity for this drug.

Supplementary Material

Refer to Web version on PubMed Central for supplementary material.

Acknowledgments

We thank Gerrit Los for his support and discussion, Eliana Beraldi, Virginia Yago and Estelle Li for technical assistance. This study was supported by l'Association pour la Recherche sur le Cancer (France), the Canadian Institutes of Health Research and Pfizer Global Research & Development (United States).

Bibliography

1. Jemal A, Siegel R, Ward E, Murray T, Xu J, Smigal C, et al. Cancer statistics, 2006. CA Cancer J Clin. 2006; 56:106–30. [PubMed: 16514137]
2. Kyprianou N, English HF, Isaacs JT. Programmed cell death during regression of PC-82 human prostate cancer following androgen ablation. Cancer Res. 1990; 50:3748–53. [PubMed: 2340521]

3. Gleave ME, Bruchovsky N, Moore MJ, Venner P. Prostate cancer: 9. Treatment of advanced disease. CMAJ. 1999; 160:225–32. [PubMed: 9951446]
4. Moreau JP, Delavault P, Blumberg J. Luteinizing hormone-releasing hormone agonists in the treatment of prostate cancer: a review of their discovery, development, and place in therapy. Clin Ther. 2006; 28:1485–508. [PubMed: 17157109]
5. Young JC, Hartl FU. Polypeptide release by Hsp90 involves ATP hydrolysis and is enhanced by the co-chaperone p23. EMBO J. 2000; 19:5930–40. [PubMed: 11060043]
6. Kamal A, Thao L, Sensintaffar J, Zhang L, Boehm MF, Fritz LC, et al. A high-affinity conformation of Hsp90 confers tumour selectivity on Hsp90 inhibitors. Nature. 2003; 425:407–10. [PubMed: 14508491]
7. Pearl LH, Prodromou C. Structure and mechanism of the Hsp90 molecular chaperone machinery. Annu Rev Biochem. 2006; 75:271–94. [PubMed: 16756493]
8. Whitesell L, Lindquist SL. HSP90 and the chaperoning of cancer. Nat Rev Cancer. 2005; 5:761–72. [PubMed: 16175177]
9. Takayama S, Reed JC, Homma S. Heat-shock proteins as regulators of apoptosis. Oncogene. 2003; 22:9041–7. [PubMed: 14663482]
10. Chiosis G, Huezo H, Rosen N, Mimnaugh E, Whitesell L, Neckers L. 17AAG: low target binding affinity and potent cell activity--finding an explanation. Mol Cancer Ther. 2003; 2:123–9. [PubMed: 12589029]
11. Vanaja DK, Mitchell SH, Toft DO, Young CY. Effect of geldanamycin on androgen receptor function and stability. Cell Stress Chaperones. 2002; 7:55–64. [PubMed: 11894840]
12. Saporita AJ, Ai J, Wang Z. The Hsp90 inhibitor, 17-AAG, prevents the ligand-independent nuclear localization of androgen receptor in refractory prostate cancer cells. Prostate. 2007; 67:509–20. [PubMed: 17221841]
13. Georgakis GV, Younes A. Heat-shock protein 90 inhibitors in cancer therapy: 17AAG and beyond. Future Oncol. 2005; 1:273–81. [PubMed: 16555999]
14. Solit DB, Basso AD, Olshen AB, Scher HI, Rosen N. Inhibition of heat shock protein 90 function down-regulates Akt kinase and sensitizes tumors to Taxol. Cancer Res. 2003; 63:2139–44. [PubMed: 12727831]
15. Solit DB, Zheng FF, Drobnjak M, Munster PN, Higgins B, Verbel D, et al. 17-Allylamino-17-demethoxygeldanamycin induces the degradation of androgen receptor and HER-2/neu and inhibits the growth of prostate cancer xenografts. Clin Cancer Res. 2002; 8:986–93. [PubMed: 12006510]
16. Chiosis G, Caldas Lopes E, Solit D. Heat shock protein-90 inhibitors: a chronicle from geldanamycin to today's agents. Curr Opin Investig Drugs. 2006; 7:534–41.
17. Price JT, Quinn JM, Sims NA, Vieusseux J, Waldeck K, Docherty SE, et al. The heat shock protein 90 inhibitor, 17-allylamino-17-demethoxygeldanamycin, enhances osteoclast formation and potentiates bone metastasis of a human breast cancer cell line. Cancer Res. 2005; 65:4929–38. [PubMed: 15930315]
18. Yano A, Tsutsumi S, Soga S, Lee MJ, Trepel J, Osada H, et al. Inhibition of Hsp90 activates osteoclast c-Src signaling and promotes growth of prostate carcinoma cells in bone. Proc Natl Acad Sci U S A. 2008; 105:15541–6. [PubMed: 18840695]
19. Chandarlapaty S, Sawai A, Ye Q, Scott A, Silinski M, Huang K, et al. SNX2112, a synthetic heat shock protein 90 inhibitor, has potent antitumor activity against HER kinase-dependent cancers. Clin Cancer Res. 2008; 14:240–8. [PubMed: 18172276]
20. Okawa Y, Hideshima T, Steed P, Vallet S, Hall S, Huang K, et al. SNX-2112, a selective Hsp90 inhibitor, potently inhibits tumor cell growth, angiogenesis, and osteoclastogenesis in multiple myeloma and other hematologic tumors by abrogating signaling via Akt and ERK. Blood. 2009; 113:846–55. [PubMed: 18948577]
21. Leung SY, Jackson J, Miyake H, Burt H, Gleave ME. Polymeric micellar paclitaxel phosphorylates Bcl-2 and induces apoptotic regression of androgen-independent LNCaP prostate tumors. Prostate. 2000; 44:156–63. [PubMed: 10881025]

22. Banerji U, de Bono J, Judson I, Kaye S, Workman P. Biomarkers in early clinical trials: the committed and the skeptics. Clin Cancer Res. 2008; 14:2512. author reply 3–4. [PubMed: 18413847]
23. Workman P, Burrows F, Neckers L, Rosen N. Drugging the cancer chaperone HSP90: combinatorial therapeutic exploitation of oncogene addiction and tumor stress. Ann N Y Acad Sci. 2007; 1113:202–16. [PubMed: 17513464]
24. Gleave ME, Hsieh JT, Wu HC, von Eschenbach AC, Chung LW. Serum prostate specific antigen levels in mice bearing human prostate LNCaP tumors are determined by tumor volume and endocrine and growth factors. Cancer Res. 1992; 52:1598–605. [PubMed: 1371718]
25. Franzoso G, Carlson L, Xing L, Poljak L, Shores EW, Brown KD, et al. Requirement for NF-kappaB in osteoclast and B-cell development. Genes Dev. 1997; 11:3482–96. [PubMed: 9407039]
26. Boyle WJ, Simonet WS, Lacey DL. Osteoclast differentiation and activation. Nature. 2003; 423:337–42. [PubMed: 12748652]
27. Miyazaki T, Sanjay A, Neff L, Tanaka S, Horne WC, Baron R. Src kinase activity is essential for osteoclast function. J Biol Chem. 2004; 279:17660–6. [PubMed: 14739300]
28. Hollingshead M, Alley M, Burger AM, Borgel S, Pacula-Cox C, Fiebig HH, et al. In vivo antitumor efficacy of 17-DMAG (17-dimethylaminoethylamino-17-demethoxygeldanamycin hydrochloride), a water-soluble geldanamycin derivative. Cancer Chemother Pharmacol. 2005; 56:115–25. [PubMed: 15791458]
29. Sydor JR, Normant E, Pien CS, Porter JR, Ge J, Grenier L, et al. Development of 17-allylamino-17-demethoxygeldanamycin hydroquinone hydrochloride (IPI-504), an anti-cancer agent directed against Hsp90. Proc Natl Acad Sci U S A. 2006; 103:17408–13. [PubMed: 17090671]
30. Glaze ER, Lambert AL, Smith AC, Page JG, Johnson WD, McCormick DL, et al. Preclinical toxicity of a geldanamycin analog, 17-(dimethylaminoethylamino)-17-demethoxygeldanamycin (17-DMAG), in rats and dogs: potential clinical relevance. Cancer Chemother Pharmacol. 2005; 56:637–47. [PubMed: 15986212]
31. Eccles SA, Massey A, Raynaud FI, Sharp SY, Box G, Valenti M, et al. NVP-AUY922: a novel heat shock protein 90 inhibitor active against xenograft tumor growth, angiogenesis, and metastasis. Cancer Res. 2008; 68:2850–60. [PubMed: 18413753]
32. Goltzman D. Mechanisms of the development of osteoblastic metastases. Cancer. 1997; 80:1581–7. [PubMed: 9362425]
33. Quinn JMW, Nakamura A, Docherty S, et al. Inhibition of chaperonin Hsp90 stimulates osteoclastogenesis *in vitro* and increases bone destruction by invading breast cancer cells. J Bone Miner Res. 2003; 18:S348.
34. Eustace BK, Sakurai T, Stewart JK, Yimlamai D, Unger C, Zehetmeier C, et al. Functional proteomic screens reveal an essential extracellular role for hsp90 alpha in cancer cell invasiveness. Nat Cell Biol. 2004; 6:507–14. [PubMed: 15146192]
35. Pratt WB, Toft DO. Regulation of signaling protein function and trafficking by the hsp90/hsp70-based chaperone machinery. Exp Biol Med (Maywood). 2003; 228:111–33. [PubMed: 12563018]
36. Myoui A, Nishimura R, Williams PJ, Hiraga T, Tamura D, Michigami T, et al. C-SRC tyrosine kinase activity is associated with tumor colonization in bone and lung in an animal model of human breast cancer metastasis. Cancer Res. 2003; 63:5028–33. [PubMed: 12941830]
37. Yoneda T, Sasaki A, Dunstan C, Williams PJ, Bauss F, De Clerck YA, et al. Inhibition of osteolytic bone metastasis of breast cancer by combined treatment with the bisphosphonate ibandronate and tissue inhibitor of the matrix metalloproteinase-2. J Clin Invest. 1997; 99:2509–17. [PubMed: 9153295]
38. Soysa NS, Alles N. NF-kappaB functions in osteoclasts. Biochem Biophys Res Commun. 2009; 378:1–5. [PubMed: 18992710]
39. Soysa NS, Alles N, Shimokawa H, Jimi E, Aoki K, Ohya K. Inhibition of the classical NF-kappaB pathway prevents osteoclast bone-resorbing activity. J Bone Miner Metab. 2009; 27:131–9. [PubMed: 19172225]
40. Iotsova V, Caamano J, Loy J, Yang Y, Lewin A, Bravo R. Osteopetrosis in mice lacking NF-kappaB1 and NF-kappaB2. Nat Med. 1997; 3:1285–9. [PubMed: 9359707]

41. Locke JA, Guns ES, Lubik AA, Adomat HH, Hendy SC, Wood CA, et al. Androgen levels increase by intratumoral de novo steroidogenesis during progression of castration-resistant prostate cancer. Cancer Res. 2008; 68:6407–15. [PubMed: 18676866]

42. Knudsen KE, Scher HI. Starving the addiction: new opportunities for durable suppression of AR signaling in prostate cancer. Clin Cancer Res. 2009; 15:4792–8. [PubMed: 19638458]

43. Magklara A, Brown TJ, Diamandis EP. Characterization of androgen receptor and nuclear receptor co-regulator expression in human breast cancer cell lines exhibiting differential regulation of kallikreins 2 and 3. Int J Cancer. 2002; 100:507–14. [PubMed: 12124798]

44. Brawer MK, Lange PH. Prostate-specific antigen and premalignant change: implications for early detection. CA Cancer J Clin. 1989; 39:361–75. [PubMed: 2482117]

45. Stamey TA, Kabalin JN, Ferrari M, Yang N. Prostate specific antigen in the diagnosis and treatment of adenocarcinoma of the prostate. IV. Anti-androgen treated patients. J Urol. 1989; 141:1088–90. [PubMed: 2468797]

46. Georget V, Terouanne B, Nicolas JC, Sultan C. Mechanism of antiandrogen action: key role of hsp90 in conformational change and transcriptional activity of the androgen receptor. Biochemistry. 2002; 41:11824–31. [PubMed: 12269826]

47. Oikonomopoulou K, Soosaipillai A, Diamandis EP. Evaluation of prostate-specific antigen as a novel biomarker of Hsp90 inhibition. Clin Biochem. 2009; 42:1705–12. [PubMed: 19632215]

48. Oudard S, Banu E, Beuzeboc P, Voog E, Dourthe LM, Hardy-Bessard AC, et al. Multicenter randomized phase II study of two schedules of docetaxel, estramustine, and prednisone versus mitoxantrone plus prednisone in patients with metastatic hormone-refractory prostate cancer. J Clin Oncol. 2005; 23:3343–51. [PubMed: 15738542]

49. Scher HI, Warren M, Heller G. The association between measures of progression and survival in castrate-metastatic prostate cancer. Clin Cancer Res. 2007; 13:1488–92. [PubMed: 17332293]

50. Kaarbo M, Mikkelsen OL, Malerod L, Qu S, Lobert VH, Akgul G, et al. PI3K-AKT-mTOR pathway is dominant over androgen receptor signaling in prostate cancer cells. Cell Oncol. 2010; 32:11–27. [PubMed: 20203370]

STATEMENT OF TRANSLATIONAL RELEVANCE

Hsp90 is a central “node” for several signaling pathways which are known to modulate prostate cancer (PCa) progression to castrate resistant stage (CRPC). Although Hsp90 inhibitor, 17-AAG is currently in clinical trials, it induces osteoclastogenesis and cannot be used in metastasis diseases. In this study we tested the activity of a novel Hsp90 inhibitor, PF-04929473 and found that it is more potent than 17-AAG, inhibits PCa cell growth and induces apoptosis. PF-04928473 inhibits both AR and AKT pathways via its ability to induce their degradation. In contrast to 17-AAG, PF-04928473 inhibits NF-κB and Src activities thereby abrogating osteoclastogenesis. PF-04929473 delays progression to CRPC in vivo without altering circulating PSA levels. These results suggest that PSA is not a good surrogate marker for anticancer activity of PF-04929473. Together, data support that targeting Hsp90 using PF-04928473 could be considered as a therapeutic strategy for CRPC with bone metastasis.

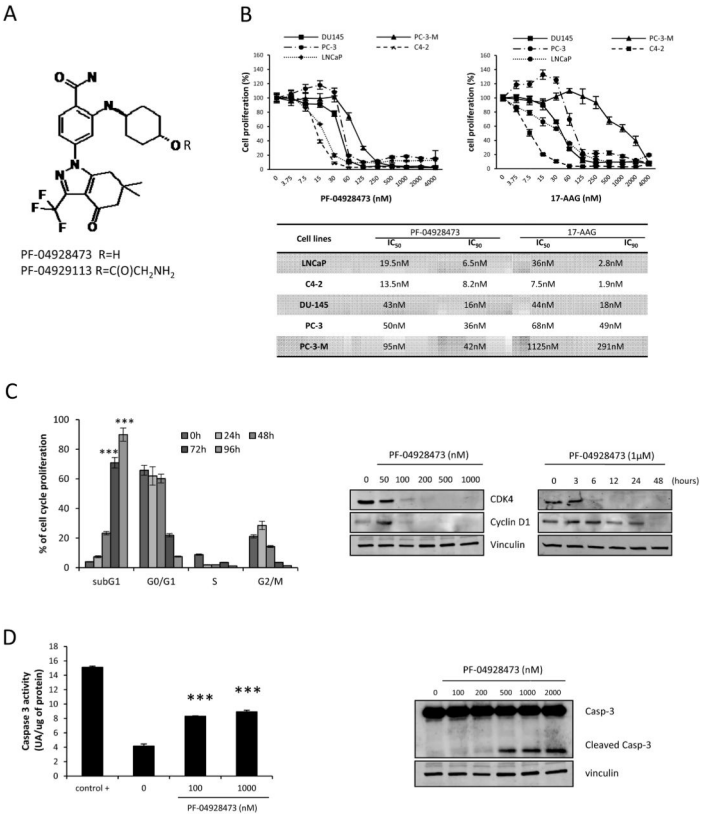

Figure 1. PF-04928473 inhibits cell growth and induces apoptosis in prostate cancer cell lines

A, chemical structure of PF-04928473 (active molecule) and PF-04929113 (pro-drug). *B*, tumor cell lines (LNCaP, C4-2, DU145, PC-3 and PC-3-M) were cultured for 72 hours in the presence of PF-04928473 or 17-AAG at the indicated concentration and cell growth was determined by crystal violet assay and compared with control. The table compares the IC_{50} and IC_{90} of each tumor cell lines between PF-04928473 and 17-AAG. *C, left*, LNCaP cells were treated with 1µM of PF-04928473 for 2 days, and the proportion of cells in $subG_1$, G_0-G_1, S, G_2-M was determined by propidium iodide staining. *C, right*, LNCaP cells were treated with PF-04928473 at indicated concentration for 2 days, and CDK4 and cyclin D1 expression levels were measured by Western blotting. *D, left*, LNCaP cells were cultured in presence of 1µM PF-04928473 for 2 days. Caspase-3 activity was determined on the cell lysates and the results are expressed in arbitrary units and corrected for protein content. ***, $p<0.001$. *D, right*, LNCaP cells were treated with 1µM PF-04928473 for 2 days and Caspase 3 expression level was assessed by Western blotting. All experiments were repeated at least thrice.

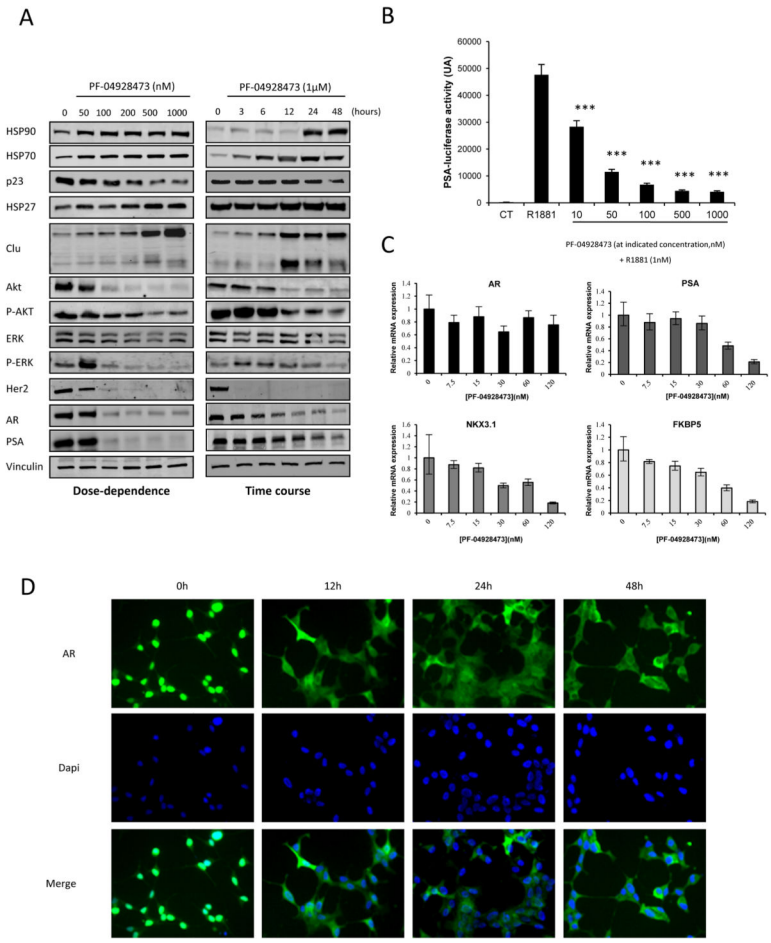

Figure 2. PF-04928473 induces degradation of Hsp90 client proteins, inhibits AR transactivation and nuclear translocation, and downregulates AR-regulated genes

A, LNCaP cells were cultured in presence of PF-04928473 at indicated concentration for 2 days and proteins regulated by HSP90, and HSPs expression levels were determined by Western blotting. *B*, LNCaP cells were transiently transfected with 1μg of PSA-luciferase for 24h, followed 1nM R1881 treatment for 12h in media supplemented with CSS and luciferase activity was determined and expressed in arbitrary units. ***, p<0.001. *C*, LNCaP cells were treated with increasing concentrations of PF-04928473 for 2 days and AR, PSA, NKX3.1 and FKBP5 mRNA levels were determined by quantitative RT-PCR. mRNA levels were normalized to level of GAPDH mRNA and expressed as mean ± SE. *D*, LNCaP cells were treated with 1μM PF-04928473 for indicated time and 0.1nM R1881 for 12h and AR localization was assessed by immunofluorescence staining. Nucleus was stained with DAPI. All experiments were repeated at least thrice.

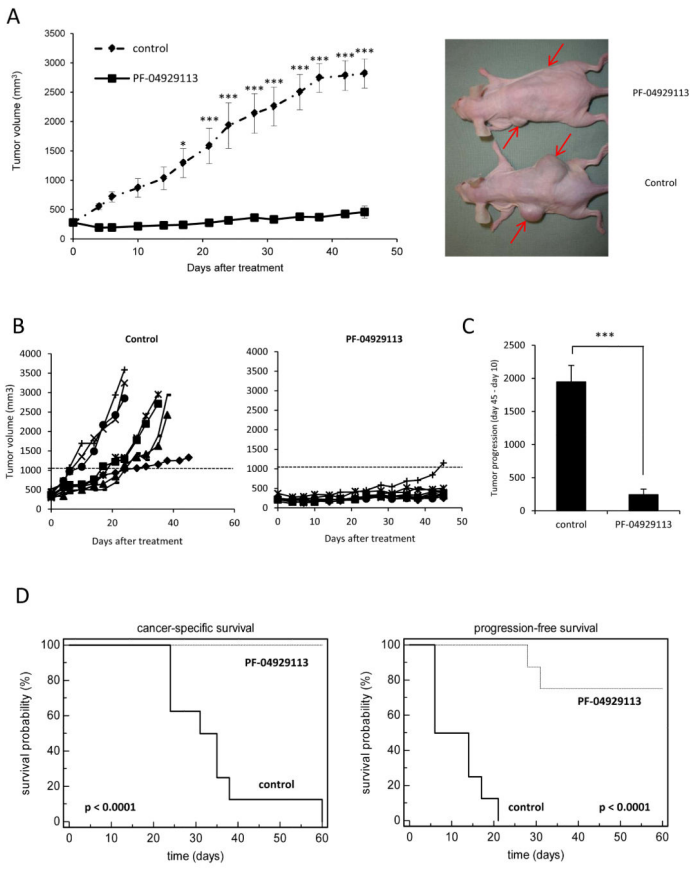

Figure 3. PF-04929113 significantly delays castrate-resistant LNCaP tumor growth and prolongs cancer specific survival

Mice were orally treated with 50mg/kg PF-04929113 three times per week, starting when serum PSA values relapsed to pre-castration levels as described in Materials and Methods. The mean (*A*) or the individual (*B*) tumor volume of mice treated was compared ± SE (n=8). *, $p<0.05$; ***, $p<0.001$. *C*, the tumor progression was estimated as the relative tumor volumes (RTV) calculated from the formula: RTV = (V_{45}/V_{10}) where V_{45} is the mean tumor volume at day 45 and V_{10} is the mean tumor volume at day 10. ***, $p<0.001$. *D*, in Kaplan-Meier curves, cancer-specific survival (*left*) and progression-free survival (*right*) were compared between mice treated with PF-04929113 and control over a 60-d period. $p<0.001$. Progression-free survival was defined as time for the first tumor volume doubling.

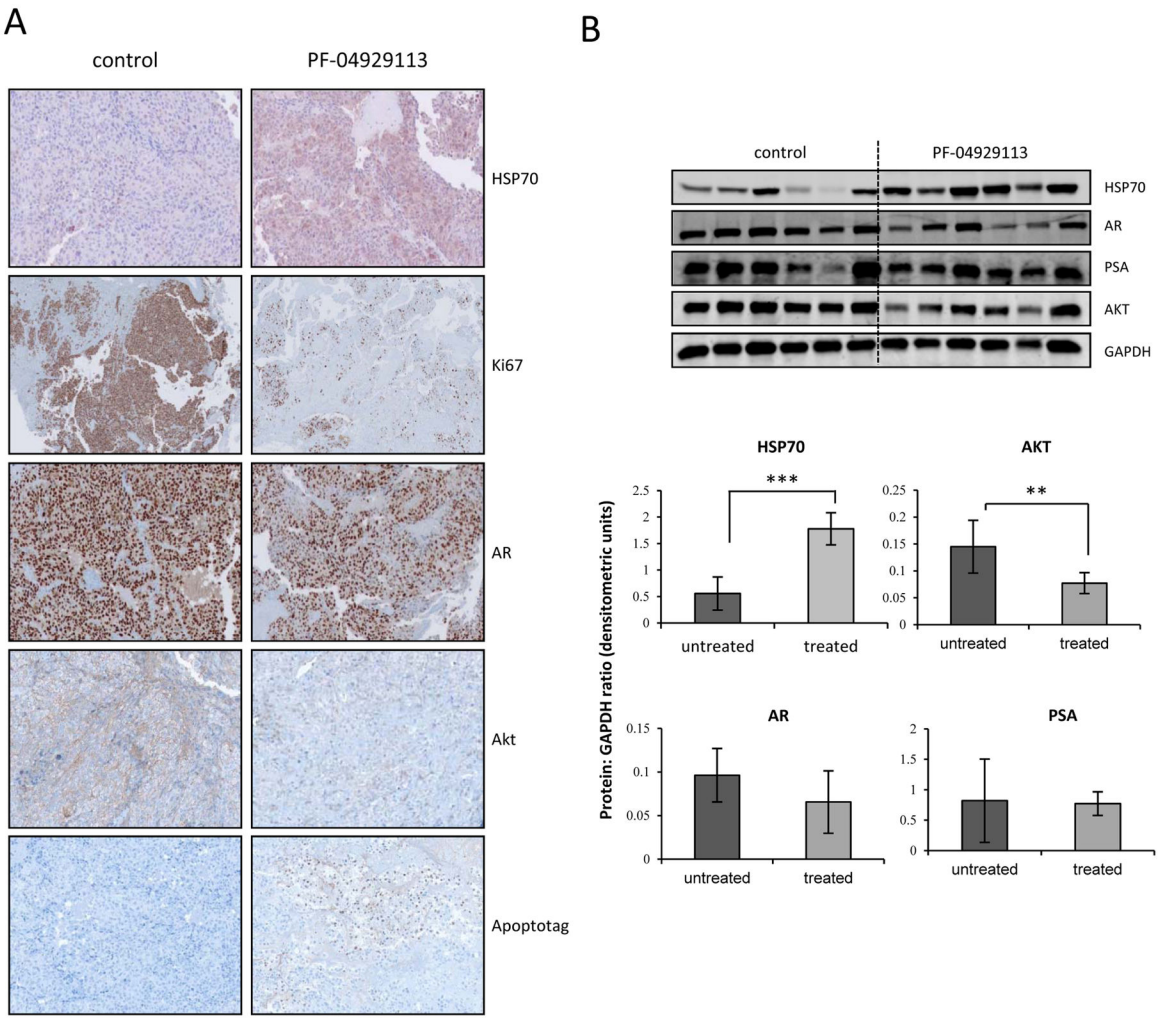

Figure 4. PF-04929113 inhibits several signaling pathways and induces apoptosis in CRPC LNCaP tumors *in vivo*

A, tumors were collected after 40 days and AR, AKT, HSP70, Ki67 and Apoptotag were evaluated by immunohistochemical analysis. *B*, total proteins were extracted from the xenograft tumors and AR, Akt and Her2 were analyzed by Western blotting. The relative levels were normalized with GAPDH and estimated in densitometric units. **, $p<0.01$.

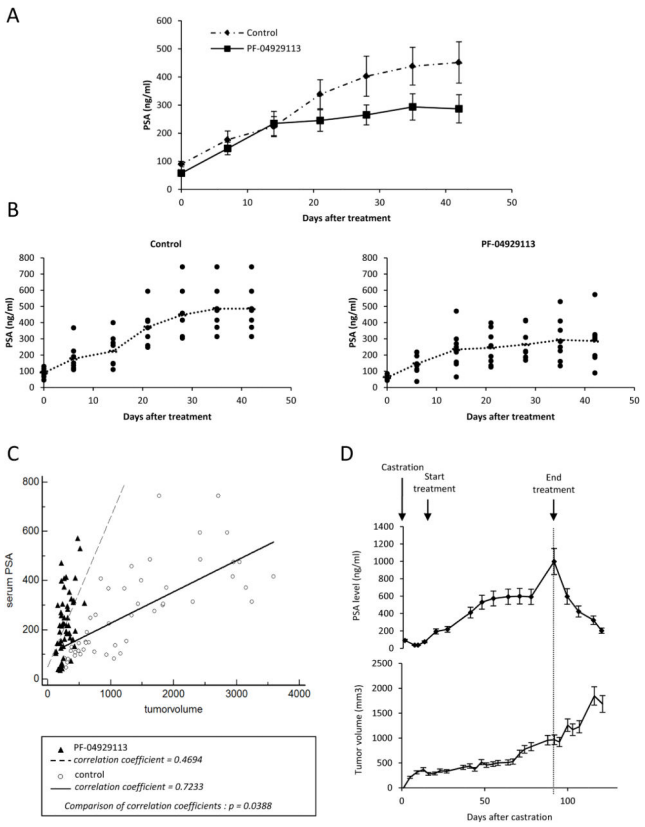

Figure 5. Serum PSA changes in PF-04929113-treated mice do not correlate to suppression of tumor volume progression

Serum samples were obtained from the tail vein of the mice once weekly to measure serum PSA by ELISA and showed as a mean PSA levels (*A*) or individual PSA level (*B*) ± SE from the first day of treatment. *C*, serum PSA progression from treated mice is not correlated to tumor volume progression ($r = 0.4694$) and significantly different of control serum PSA which increases proportionally to tumor volume with a high degree of correlation ($r = 0.7233$). *D*, the relationship between the serum PSA and tumor volume of mice treated with PF-04929113 from the castration time to the sacrifice of mice ± SE.

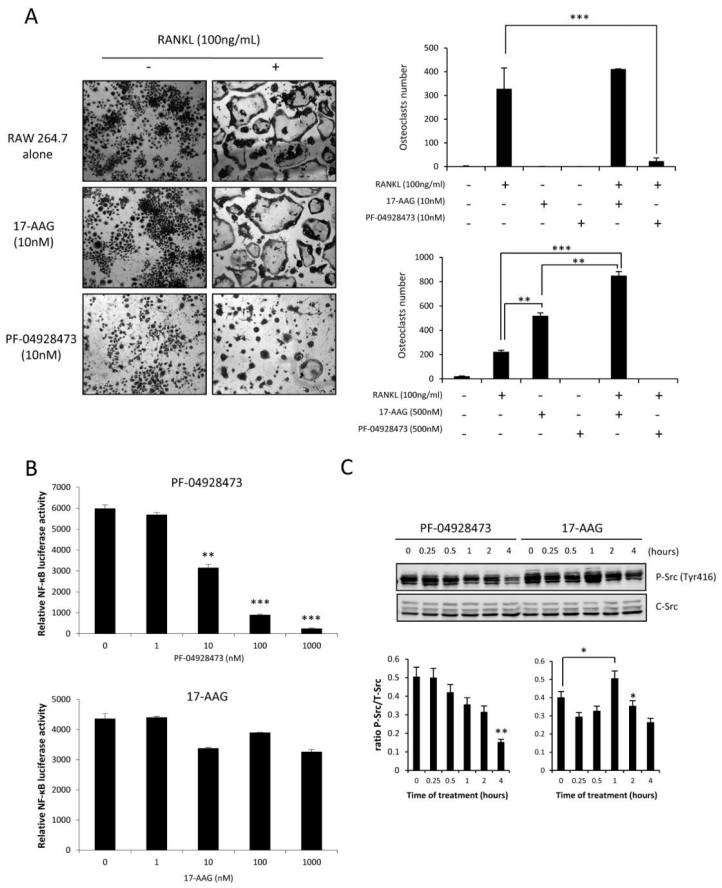

Figure 6. PF-04928473 inhibits osteoclastogenesis

A, Osteoclastogenesis was determined by MGG staining. Raw 264.7 osteoclast precursors were cultured for 5 days in the presence of 100 ng/mL of RANKL with or without 10 nM of PF-04928473 or 17-AAG. Multinucleated cells were counted and compared between all conditions ± SD. ***, $p<0.001$. *B*, PF-04928473 inhibits NF-KB transactivation. Raw 264.7 cells were transiently transfected with NF-KB-Luc and Renilla plasmids. After 48 hours and stimulation with 20 ng/ml TNF-α, cells were harvested and luciferase activity was determined. *C*, Raw 264.7 cells were treated with RANKL for 5 days and then treated with 1μM PF-04928473 or 17-AAG for indicated time. Total lysates were analyzed by western blotting using total-Src and p-Src antibodies. Western blots were quantitated using using Odyssey infrared imaging system application software version 3.0. All experiments were repeated at least thrice. *, $p<0.05$; **, $p<0.01$.